

Measuring breathing induced oesophageal motion and its dosimetric impact

T. Fechter^{1,2}, S. Adebahr^{2,3}, A.-L. Grosu^{2,3} and D. Baltas^{1,2}

¹ Division of Medical Physics, Department of Radiation Oncology, Medical Center – University of Freiburg, Faculty of Medicine. University of Freiburg, Germany

² German Cancer Consortium (DKTK). Partner Site Freiburg, Germany

³ Department of Radiation Oncology, Medical Center – University of Freiburg, Faculty of Medicine. University of Freiburg, Germany

E-mail: tobias.fechter@uniklinik-freiburg.de

Abstract. Stereotactic body radiation therapy allows for a precise and accurate dose delivery. Organ motion during treatment bears the risk of undetected high dose healthy tissue exposure. An organ very susceptible to high dose is the oesophagus. Its low contrast on CT and the oblong shape renders motion estimation difficult. We tackle this issue by modern algorithms to measure the oesophageal motion voxel-wise and to estimate motion related dosimetric impact. Oesophageal motion was measured using deformable image registration and 4DCT of 11 internal and 5 public datasets. Current clinical practice of contouring the organ on 3DCT was compared to timely resolved 4DCT contours. The dosimetric impact of the motion was estimated by analysing the trajectory of each voxel in the 4D dose distribution. Finally an organ motion model was built, allowing for easier patient-wise comparisons. Motion analysis showed mean absolute maximal motion amplitudes of 4.24 ± 2.71 mm left-right, 4.81 ± 2.58 mm anterior-posterior and 10.21 ± 5.13 mm superior-inferior. Motion between the cohorts differed significantly. In around 50 % of the cases the dosimetric passing criteria was violated. Contours created on 3DCT did not cover 14 % of the organ for 50 % of the respiratory cycle and the 3D contour is around 38 % smaller than the union of all 4D contours. The motion model revealed that the maximal motion is not limited to the lower part of the organ. Our results showed motion amplitudes higher than most reported values in the literature and that motion is very heterogeneous across patients. Therefore, individual motion information should be considered in contouring and planning.

Keywords: Intra-fraction motion, Oesophagus, Lung cancer, SBRT, 4DCT, 4D Dose, Deformable image registration

1. Introduction

Modern stereotactic body radiation therapy (*SBRT*) in the thoracic region allows for a precise and accurate dose delivery. The steep dose gradients that are possible with SBRT facilitate a dose boost in the target volume while sparing the organs at risk (*OARs*). However, during treatment it is possible that certain OARs move due to e.g. respiration, heart beat, swallowing or intrinsic movements leading to the risk of undetected OAR-exposure to the high dose field. An OAR that requires special care when treating tumours in or close to the mediastinal region is the oesophagus. Its radiosensitive mucosa making it susceptible to injuries due to higher dose exposure. Thus, sometimes severe sequelae as oesophagitis, hemorrhagia, fistula with mediastinitis or strictures can occur. Consequently great caution has been exercised implementing SBRT to central regions, especially to lesions in proximity to the oesophagus (Timmerman et al. 2006, Adebahr et al. 2015), as for SBRT - applying huge biological effective dose to the tissue - mediastinal tolerance doses are not known. Several retrospective data suggest dosimetric constraints (e.g. Adebahr et al. 2015). However, it is not clear what dose really leads to severe harm to the oesophagus. Thus, it is necessary to keep the oesophagus out of the high dose irradiation field. Therefore a precise definition of the organ's boundaries and an estimation of its motion is required.

The current approach to demarcate the oesophagus for treatment planning is to delineate its outline on ungated computed tomography (*CT*) or on average CT images (computed on basis of 4DCT) (Kong et al. 2011). This procedure has two drawbacks. First, a precise organ outline is not possible due to the blurriness of average CT or the motion artifacts in ungated CT. Second, ungated CT does not allow for an estimation of organ motion at all, on average CT the motion can only be guessed from the motion blur. The motion information from a time gated CT acquisition (*4DCT*) is usually considered only for the target volume itself but neglected for OARs as it would be an elaborate and time consuming procedure. Automatic contouring could alleviate motion consideration of OARs but developing automatic methods for contouring the oesophagus is a difficult task because its often hardly distinguishable from surrounding structures and sometimes even experts have difficulties defining reliably its boundaries resulting in a high inter observer variability (Collier et al. 2003). However, during the last years deep learning algorithms have been presented for solving this task (Fechter et al. 2017, Isensee et al. 2019, Yang et al. 2018, Lambert et al. 2019). Some of these methods are able to produce results within the inter-rater variability (Collier et al. 2003). A supportive usage of these methods in the clinic could enable a full exploit of the 4DCT motion information to generate time resolved contours of the oesophagus.

Motion estimation of the oesophagus has been the scope of several publications with a multitude of applied techniques and heterogeneous results. In the publications by Gao et al. (2019) and Kobayashi et al. (2016) only the shift of the oesophageal centroid was measured using rigidly aligned 4DCT time phase images. Rigid registration was also used by Cohen et al. (2010) with a general motion analysis in a region above and a region

below the Carina. Manual measurements in combination with rigid image alignment were used by Patel et al. (2009). Sekii et al. (2018) and Doi et al. (2018) used fiducial markers to measure the oesophageal motion in 4DCT. The work by Doi et al. (2018) differentiated between upper and lower region whereas Sekii et al. (2018) analysed the motion separately for upper, middle and lower region. Deformable image registration (*DIR*) was utilised by Palmer et al. (2014) and Yaremko et al. (2008). Palmer et al. (2014) focused on heart beat induced motion, Yaremko et al. (2008) investigated the impact of respiration on oesophageal tumor positions but used only maximum inhale and exhale phase. In Weiss et al.'s (2008) work motion was estimated indirectly by measuring the distance change between the center of mass of the gross tumour volume and oesophagus during breathing for lung cancer patients. Gao et al. (2019) measured mean absolute magnitudes of oesophageal motion below 1 mm in all 3 dimensions. Median absolute maximum amplitudes from 1.9 mm to 2.4 mm anterior-posterior (*AP*), 1.0 mm to 1.8 mm left-right (*LR*) and 6.8 mm to 7.1 mm superior-inferior (*SI*) were reported by Doi et al. (2018), Sekii et al. (2018), Yaremko et al. (2008) and Kobayashi et al. (2016). Slightly higher values yielded the study by Patel et al. (2009) with 2.8 mm AP, 2.2 mm LR and 8 mm SI. An average motion of 3 mm in transversal plane was reported by Weiss et al. (2008). In Cohen et al.'s (2010) publication an average absolute displacement of 4.1 mm LR and 2.8 mm AP was reported. The average maximum oesophageal displacement due to cardiac motion is 4.7 mm LR, 4.1 mm AP and 7.0 mm SI according to Palmer et al. (2014).

We attribute the heterogeneous results to a number of points: Rigid registration as it is used by Gao et al. (2019), Kobayashi et al. (2016) and Cohen et al. (2010) can not depict the complex nature of the mediastinal soft tissue motion. Although the usage of fiducials can give very precise results for the location where the fiducial is placed, the deformation between fiducials needs to be estimated. Additionally, Sekii et al. (2018) and Doi et al. (2018) placed the fiducials only in the direct vicinity of oesophageal tumours, whereby no assertions about the whole organ can be made. Yaremko et al. (2008) deformably registered maximum inhale and exhale phase and focused only on the tumour in the oesophagus. Palmer et al. (2014) analysed only cardiac induced motion from the Carina to the bottom of the heart and is therefore not comparable.

The impact of motion on the delivered dose was addressed mainly for the tumour so far (Ehrbar et al. 2016, Rouabhi et al. 2015, Chung et al. 2018, Cai et al. 2015). That the oesophageal motion causes a deviation from the planned dose, but only within the constraints was recently shown (Wang et al. 2019). *DIR* was used to measure deformations, but solely for a small part of the organ, no timely resolved contours and a rather small number of patients.

In this work we present a method to estimate the respiration induced oesophageal motion voxel-wise for the whole organ. In addition to the motion analysis we investigate whether the current clinical practise to contour the oesophagus on a 3D CT might bear risks of missing parts of the organ or overestimating the volume, followed by a dosimetric assessment that evaluates tissue motion in a 4D dose distribution. In a last step we build

a motion model of the oesophagus allowing for a patient wise motion comparison and an illustration of the motion not limited to predefined regions. The contributions of this work allow to estimate over or under dosage due to motion and might thus contribute to lower motion induced uncertainties and consequently even facilitate SBRT of tumours closer to the oesophagus.

2. Data

Oesophageal motion was analysed for 11 internal (*C1* - *C11*) datasets and 5 external (*T1* - *T5*) datasets from The Cancer Imaging Archive. Each of them consisting of a 4D retrospectively respiratory gated CT acquisition consisting of 10 3D phase images. In addition the 11 internal datasets had an average CT and information about the delivered dose in terms of 3D and 4D dose matrices. 9 of the 16 datasets depicted the whole organ, 3 showed the oesophagus in the total lung region, on 2 datasets the central part was visible, 1 dataset showed the lower and 1 dataset the upper part of the oesophagus. The minimum depicted length was 180 mm.

2.1. Internal Datasets

The 11 clinical datasets were acquired on a Gemini TF Big Bore or Gemini Brilliance Big Bore (Philips Healthcare, Andover, MA, USA), with voxel resolution 0.97×0.97 mm - 1.17×1.17 mm in axial plane and 2.00 mm in z-direction. Volumes have 90 - 114 slices, each slice of size 512×512 voxels. All patient suffered from central non-small-cell lung cancer (*NSCLC*), received 60 Gy in 8 fractions of 7.5 Gy. Dose prescription was chosen such that 95 % of the PTV received at least the nominal fraction dose, and 99 % of the PTV received a minimum of 90 % of the nominal dose (according to ICRU *Report 83* 2016). For dosimetric analysis we used 11 dose matrices per patient. The baseline dose, which represents current clinical practice, was determined by calculating the delivered dose on the basis of average CT (*3DDose*). In addition, to measure the impact of tissue motion and the associated change in physical properties, the applied dose was recalculated (with same beam configuration and without new optimisation) for each time phase CT separately creating a 4D dose volume (*4DDose*). Each time-phase dose representing a tenth of the total dose (Rouabhi et al. 2015). The temporal schedule of dose delivery was neglected. Dose calculations were done with Eclipse treatment planning software v.15.6 (Varian Medical Systems, Palo Alto, CA, USA). The study was approved by the local ethics committee.

2.2. The Cancer Imaging Archive Datasets

The external datasets were retrieved from the 4D-Lung collection (Hugo et al. 2016) containing locally advanced NSCLC patients available at The Cancer Imaging Archive (*TCIA*) (Clark et al. 2013). All taken datasets consisted of a 4D fan beam CT scan acquired on a 16-slice helical CT scanner (Brilliance Big Bore, Philips Healthcare,

Andover, MA, USA) divided into 10 breathing phases and oesophagus contours for each time phase created by a single Radiation Oncologist. For our analysis we used the patients 100, 101, 102, 103 and 107. Only for those patients 4D oesophagus contours were available. Voxel spacing was $0.97 \times 0.97 \times 3$ mm in x-, y- and z-direction. Each CT slice consisted of 512×512 voxels. The number of slices ranged from 84 to 149.

3. Methods

To accomplish the goals defined in the introduction we need to preprocess the datasets, then identify the oesophagus on each time phase and average CT scan by segmenting the images and eventually calculating trajectories by DIR.

3.1. Preprocessing

Image registration of 4D datasets is a very elaborate task. To reduce the amount of data to be processed every dataset was cropped to a region of interest (*ROI*). After the oesophagus contours were completed the rectangular cuboid shaped ROI was defined as follows: combine all time phase contours and the average CT contour with a logical OR operator to a union contour, subsequently determine the minimum and maximum positions of the union contour in x-, y- and z-direction, finally add a margin of 20 voxels on each side. In the course of this work we tried different margins. A margin of 20 voxels is a good trade-off between including all relevant structures and faster image processing. For dosimetric analysis we re-sampled the dose to image resolution with Plastimatch v.1.7 (<http://www.plastimatch.org/>) and tri-linear interpolation.

For the creation of the inter patient motion model the maximum inhale datasets were re-sampled to the resolution of one reference dataset (Case 100 of TCIA) after affine registration with elastix's (Klein et al. 2010) third order B-spline interpolation.

3.2. Segmentation

The oblong shape and the poor contrast to surrounding tissue render the delineation of the oesophagus a time-consuming task. Therefore, we employed our recently developed CNN-based algorithm for automatic oesophagus delineation (Fechter et al. 2017) to create an initial contour on each 3D time phase image and the average CT of the internal datasets. The generated contours were then checked and manually corrected by one observer and double-checked by an experienced radiation oncologist. The final 121 reference contours follow the EORTC 22113-08113 Lungtech protocol and guidelines (Kong et al. 2011, Adebahr et al. 2015). For the external datasets the contours provided by TCIA were used. Manual contouring and visual inspection was done with 3D Slicer v.4.10.0 (Fedorov et al. 2012).

3.3. Registration

In this project inter-patient and intra-patient registration were conducted. Intra-patient registration was used to measure the oesophageal motion for each patient and inter-patient registration to create the motion model. In a 4DCT the time phase images are already rigidly aligned by the scanner therefore solely DIR was needed for the intra-patient registration, whereas for inter-patient alignment affine and deformable registration were necessary.

Elastix (Klein et al. 2010) was used for affine image registration with the settings provided for CT lung registration with mutual information (Par0003 available at http://elastix.bigr.nl/wiki/index.php/Parameter_file_database presented in the work by Klein et al. (2010)). DIR was done with the 4D algorithm by Fechter & Baltas (2020) which is able to consider the underlying cyclic respiratory motion pattern. In this work we further extended the algorithm by a diffeomorphic layer for the reduction of anatomically implausible deformations and the option to make use of segmentation information to steer the registration process. The code is available online (<https://github.com/ToFec/OneShotImageRegistration>).

For the intra-patient registration we used solely CT data and no contour information. Preliminary experiments showed that using the contour information reduces the accuracy due to slight contour inconsistencies. The inter-patient registration is more challenging due to anatomical variations between patients. Therefore we had, after the affine registration with Elastix, to make use of CT as well as contour information (in terms of distance maps) for DIR. For the patients C4 and C10 acceptable results could only be generated with contour based information, neglecting CT volume information because of anatomical differences.

After a general evaluation (see 4.1) of the registration algorithm, the quality of inter- and intra-patient registration was evaluated manually by considering anatomical landmarks and deformation vector field (*DVF*) properties.

3.4. Evaluation

To evaluate the similarity between contours we considered 3 methods. Volume similarities are measured by the Sørensen-Dice index (*DSC*) (Sørensen 1948). Volume-based metrics alone might miss clinically relevant differences as they show a lower sensitivity to errors where outlines deviate and the volume of the erroneous region is small compared to the total volume. Thus, we considered also distance-based metrics like the Hausdorff distance (HD) and the average symmetric surface distance (ASSD). DSC, HD and ASSD were calculated using MedPy v.0.4.0 (<https://pypi.org/project/MedPy/>).

To compare dose matrices we used the gamma analysis (Low et al. 1998) provided by Plastimatch v.1.7. The gamma criterion at a given position is calculated by comparing the dose value in the reference dose matrix to the dose values within a given range in the other dose matrix. If the gamma value is below or equal to one the dose values

at a given position are equal or differ by an acceptable amount in a given range. In our experiments we calculated the local gamma index in two different ways: First, we followed the recommendations by the AAPM (Miften et al. 2018) with a passing criteria of 3%/2mm, a low dose cut-off of 10 % of the prescription dose (60 Gy) and a minimum passing rate of 90 % for acceptable deviations. As, for some of our cases, the oesophagus resides in the low dose area and a big part is cut-off with the 6 Gy threshold, we performed a second gamma experiment with weaker criteria of 3%/3mm as it is common in the literature (e.g. Hussein et al. 2017, Han et al. 2018), a low dose cut-off of 10 % of the maximum dose inside the oesophagus and a minimum passing rate of 80 % (Han et al. 2018). In addition to the gamma analyses we provide the dosimetric indices D_{max} , $D_{2\%}$, $D_{33\%}$ and $D_{50\%}$ for the oesophagus. D_{max} is the maximal dose the organ receives, $D_{x\%}$ ($x \in \{2, 33, 50\}$) gives the dose received by at least $x\%$ of the volume.

Statistical analysis was performed with the Wilcoxon signed-rank test. This test, which has for null hypothesis that the median group difference is zero, was chosen due to non-normal distribution and heteroscedasticity of the data. In our experiments, the confidence alpha was set to 5 %.

3.5. Mathematical Notation

Let I^N be a 4D image dataset consisting of N 3D images. In this work three types of image datasets were used: CT volumes, dose matrices and contours in binary image representation. The DIR algorithm yields a transformation T^N that maps each 3D image I_n in I^N to its timely adjacent successor I_{n+1} (as we deal with periodic data I_{N-1} is aligned to I_0). T^N consists of N 3D dense vector fields and describes the trajectory for each voxel in I^N . $T_i^j(x)$ is the sequential application of the deformation fields T_i to T_j to the position of voxel x .

4. Experiments

4.1. Registration QA

To ensure that the extended version of the used DIR algorithm is as accurate as the published version we applied the algorithm to the maximum inhale and exhale CT scans of publicly available POPI and DirLab datasets (Vandemeulebroucke et al. 2011, Castillo, Castillo, Martinez, Shenoy & Guerrero 2009, Castillo, Castillo, Guerra, Johnson, McPhail, Garg & Guerrero 2009). Both provide landmarks for quality assurance. We used these datasets also in our original work, so we are able to infer directly the impact of the algorithm modifications. In addition, to ensure that the registration results of aligning the maximum inhale and exhale phase (*3D registration*), which was done for the POPI and DirLab experiment, are comparable to the alignment of all consecutive time phases in a 4D dataset (*4D registration*), we used the calculated DVFs to propagate the oesophagus contours over time. First with the 4D DVF and

then with the 3D DVF. The propagated contours were compared at common time phase images (maximum inhale and exhale) with DSC, HD and ASSD.

4.2. Comparison of Contouring Methods:

The current clinical practice to contour OARs on average or ungated CT acquisitions bears the risk that relevant organ motion is either averaged out or not recorded. For this reason, we compared the oesophagus contours delineated on 4DCT, which depict the motion, to the volumes delineated on the average CT images. In a first step we created 11 4D contour sums S^{N+1} for each patient. First by simply summing up the contours drawn on each time phase image on the 4DCT. The remaining 10 'motion adapted' sums S^N were created by propagating the contour drawn on one time phase I_i to all other time phases with the DVFs and a summation of the propagated contours:

for all $i \in N$ do:

- 1) initialise S_i with I_i
- 2) set j to $i + 1$
- 3) deform I_i with T_i^j and add result to S_i
- 4) if $j < N - 1$ set j to $j + 1$ otherwise set j to 0
- 5) if j is equal to i *continue* with next i otherwise go to 3)

The add operation in 3) is performed voxel wise as all I_n in I^N have the same dimension, voxel size and origin. Binary image representation (0: background, 1: foreground) of the contours was used for the calculations.

In a second step the coverage of the contours drawn on the 4DCT by the contour drawn on the average CT was measured by calculating DSC, HD and ASSD between the contour delineated on the average CT and all $S_n \in S^{N+1}$. For this we had to normalise S^{N+1} by setting all voxel values above 1 to 1.

In a third step we estimated voxel wise the time (in fractions of the respiratory cycle) oesophageal tissue is not covered by the contour of the average CT by masking all $S_n \in S^{N+1}$ with the average CT contour. The value of a voxel in a masked sum image indicates in how many time phases oesophageal tissue is present at the coordinates of the respective voxel but not covered by the contour of the average CT.

The repetition of the experiment 11 times (for each $S_n \in S^{N+1}$) was done to mitigate the influence of uncertainties in the contouring and to investigate whether the 4D contours are reflected by the calculated DVFs. Only the internal datasets contain contours for the average CT, therefore this experiment was restricted to the 11 patients of the internal cohort.

4.3. Dose and Oesophagus Motion Analysis:

In the following we describe at first how the impact of organ motion on the calculated dose was estimated, followed by the details of the voxel wise motion analyses.

As mentioned above, each time phase of the 4DDose contains a fraction of the delivered dose. To facilitate a comparison with the 3DDose of the average CT, we had to map the 4DDose back to a 3DDose volume under consideration of the DVF motion information. A motion corrected 3DDose volume M_i was created by summing up the dose values in the 4DDose I^N along a voxels trajectory given by the DVF, starting from I_i . For every $I_i \in I^N$ one motion corrected dose M_i was created:

for all $i \in N$ do:

- 1) initialise M_i with I_i
- 2) set j to $i + 1$
- 3) for each $x \in M_i$ do $M_i(x) = M_i(x) + I_j(T_i^j(x))$
- 4) if $j < N - 1$ set j to $j + 1$ otherwise set j to 0
- 5) if j is equal to i *continue* with next i otherwise go to 3)

In the gamma analysis we compared the 3DDose to all motion corrected dose volumes M_i . The gamma analysis was done with the contour defined on the average CT. Also the dosimetric indices D_{max} , $D_{2\%}$, $D_{33\%}$ and $D_{50\%}$ were calculated for the 3DDose and all M_i but with the contour related to the respective volume under consideration.

During image acquisition the oesophagus can change its inner appearance e.g. because the patient swallows regions filled with air can appear or disappear. Such changes in the inner appearance are not necessarily connected with a change in the outer shape or position of the organ but are reflected by high amplitudes in the DVFs. To avoid that these high amplitudes which are not caused by a real positional change affect the motion statistics, only the oesophageal border region was used for motion analysis. The border region was created by subtracting the eroded contour from the original contour. The maximal motion extent for a voxel x in the oesophageal border region defined in time phase I_i was estimated by following x on its trajectory in T^N and tracking its position:

- 1) set j to $i + 1$ and amp_{max} to 0
- 2) set amp to $|x - T_i^j(x)|$
- 3) if $amp > amp_{max}$ set amp_{max} to amp
- 4) if $j < N - 1$ set j to $j + 1$ otherwise set j to 0
- 5) if j is equal to i terminate otherwise go to 2)

amp_{max} is calculated separately in x-, y- and z-direction for all border region voxels and all $I_i \in I^N$. In total 10 motion maps per patient were created.

Like in 4.2 the creation of dose matrices and motion maps for each time phase was done to account for uncertainties in contouring and registration. The motion analysis was conducted for all cases, the dose evaluation only for internal cases.

4.4. Oesophagus Motion Model:

In recent works the inter-patient oesophageal motion comparison was facilitated by means of comparing the average motion in predefined anatomical regions (Cohen et al. 2010, Sekii et al. 2018, Doi et al. 2018) or only in the region around the tumor (Yaremko et al. 2008, Wang et al. 2019). In this work we envisaged a method for a more detailed comparison on a voxel level. For this purpose we registered the maximum inhale phase of all datasets to a common reference. As reference case we chose Case 100 of TCIA because of its good image quality and it shows the whole oesophagus without any anatomical abnormalities. The maximum inhale phase proved to be the most stable one for measuring motion amplitudes. In 35 % the maximal motion amplitude was detected when using the maximum inhale phase as a reference and in the remaining 75 % the maximal motion amplitude of the maximum inhale phase deviated only by 0.88 mm from the real maximal motion amplitude. The affine registration matrix and the DVFs were then used to transfer the motion information of each patient to the reference case. This procedure allowed for a statistical motion analysis of the whole cohort on a voxel level and a visualization of the whole organ motion easy to interpret.

5. Results

5.1. Registration QA

The registration of the POPI and DirLab datasets reduced the average registration error \pm standard deviation (SD) from 1.49 ± 1.59 mm to 1.09 ± 1.27 mm compared to our previous work. The positive impact of the algorithm changes makes the new version eligible for usage in this work. The experiment for comparing 3D and 4D registration showed that the 4D registration (median DSC, HD and ASSD of 0.84, 7.78 mm and 0.94 mm) yielded slightly worse but still reasonable results compared to the 3D registration (median DSC, HD and ASSD of 0.85, 6.05 mm and 0.86 mm).

5.2. Comparison of Contouring Methods

The first point that attracts attention when comparing the oesophagus contours on 4DCT to the contour on average CT, is that the volumes of the contour sums $S_i \in S^{n+1}$ are on average 1.38 times bigger than the volume described on average CT. Average DSC, HD and ASSD \pm SD were 0.80 ± 0.04 , 10.70 ± 2.88 mm and 1.23 ± 0.31 mm, respectively. Results for each case can be found in table 1. The analysis of the masked sum images revealed that around 14 % of the oesophageal volume was outside the average contour for at least 50 % of the respiratory cycle. Figure 1 illustrates the chronological coverage of the 4D contours by the average contour.

Table 1: Overview of the contouring and motion analysis results for the 11 clinical (*C1* - *C11*) and the 5 The Cancer Imaging Archive (*T1* - *T5*) datasets. The second column gives the ratio between the 4DCT union oesophagus contours and the contour done on average CT. Columns 3 to 5 give Sørensen-Dice index (*DSC*), Hausdorff distance (*HD*) and average symmetric surface distance (*ASSD*). Columns 6 to 8 show the maximum absolute motion left-right (*LR*), anterior-posterior (*AP*) and superior-inferior (*SI*).

Data	$\frac{Vol. 4D Union}{Vol. average}$	DSC	HD (mm)	ASSD (mm)	LR (mm)	AP (mm)	SI (mm)
C1	1.37	0.82	10.73	1.19	5.30	3.77	5.57
C2	1.41	0.79	11.15	1.30	4.25	4.18	15.85
C3	1.43	0.79	12.79	1.45	4.33	4.40	5.06
C4	1.37	0.82	11.68	1.14	4.51	2.75	9.22
C5	1.22	0.84	6.83	0.89	1.06	1.06	3.41
C6	1.46	0.78	12.33	1.24	3.32	4.70	9.52
C7	1.61	0.76	8.56	1.73	4.37	4.69	8.21
C8	1.41	0.73	11.05	1.40	3.84	3.08	7.19
C9	1.31	0.80	13.81	1.16	2.57	2.58	4.05
C10	1.18	0.86	9.95	0.81	3.04	4.16	14.46
C11	1.42	0.81	8.78	1.24	3.07	4.34	6.11
T1	-	-	-	-	3.44	5.39	13.47
T2	-	-	-	-	4.70	9.83	17.07
T3	-	-	-	-	8.84	8.33	13.39
T4	-	-	-	-	6.52	10.37	20.83
T5	-	-	-	-	4.71	3.39	10.01
Mean	1.38	0.80	10.70	1.23	4.24	4.81	10.21
SD	0.21	0.04	2.88	0.31	2.71	2.58	5.13
Min	1.03	0.72	6.22	0.72	1.06	1.06	3.41
Max	1.72	0.87	17.43	1.87	8.84	10.37	20.83

5.3. Dose and Oesophagus Motion Analysis

The investigation of the motion impact on delivered dose resulted in a statistically significant different dose distribution of average CT and motion corrected dose in all cases. However, the more clinically relevant gamma comparisons showed a violation of the gamma criterion in 6 out of 11 cases for 3%/2mm/90% and in 5 out of 11 cases for 3%/3mm/80%. The maximal measured deviation of the maximum dose was 2 Gy, whereas $D_{2\%}$ varied maximally by 1 Gy. In 9 of the 11 patients D_{max} calculated with the average CT was covered by the 95 % confidence interval of the motion corrected D_{max} values. For $D_{2\%}$ this was the case for 10 of the 11 patients. In table 2 the respective values can be seen. Differences between the two gamma experiments (e.g in C9 and C11) occurred because the cut-off threshold calculated on basis of the prescription dose was close to the maximum dose inside the organ and therefore solely a small amount of voxels could be considered for calculation. For some cases, e.g. C4, the motion corrected dose showed lower and higher dose values compared to the dose distribution

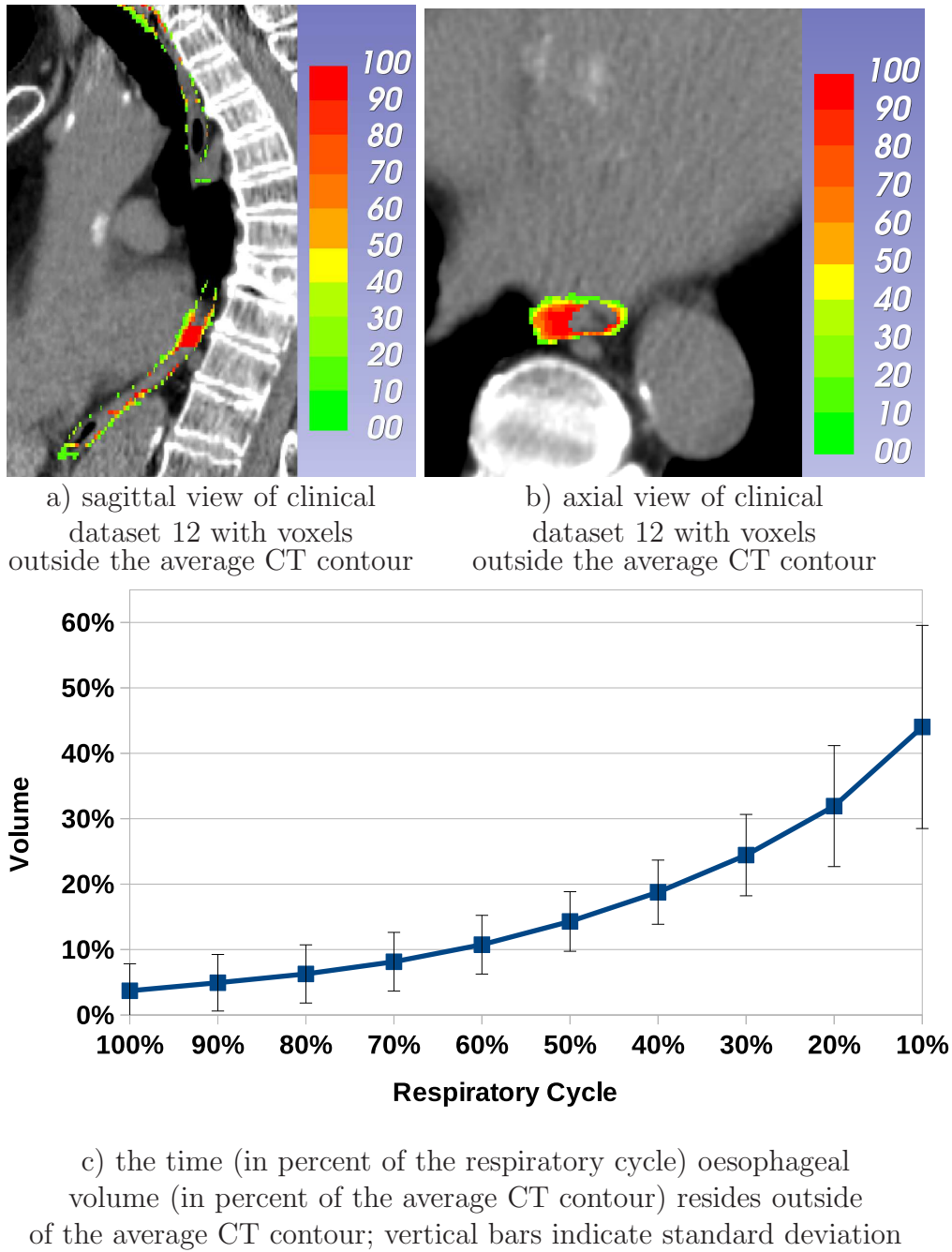


Figure 1: This figure shows oesophageal tissue that is not covered by the contour done on average CT. In a) and b) the color indicates the time (in percent of the respiratory cycle) a voxel is not covered by the average CT contour but depicts oesophageal tissue. c) shows the average over 11 cases for the volume fraction of oesophagus lying outside the contoured volume defined on the average CT for a specific fraction of the respiratory cycle.

calculated on average CT. We can attribute this phenomenon to uncertainties in the organ delineation. In Fig. 2 it is shown that the tissue motion is not reflected by the

contours and by considering just the contours, one could assume motion in a different direction.

Table 2: Dosimetric analysis for the 11 clinical (*C1* - *C11*) datasets. Column 2 shows the distance of the oesophagus from the maximum dose delivered during treatment. *D_{max} Average* lists the maximum dose values the oesophagus receives according to calculation on average CT. We calculated the motion corrected dose for each time phase contour of the 4DCT to account for contouring uncertainties. In the column *D_{max} Motion* the maximum dose range of the motion corrected dose can be seen. The columns *D_{x%}* ($x \in \{2, 33, 50\}$) give the dose received by at least $x\%$ of the volume for planned and motion corrected dose. Statistically significant differences in dose distributions between the dose calculated on average CT and of the motion corrected dose maps are marked with an asterisk. The average gamma passing rates for the local gamma analysis are given in the last two columns. The first gamma analysis had a cut-off of 10 % of the prescription dose (60 Gy), the second analysis was done with a cut-off of 10 % of the maximum dose inside the oesophagus.

Data	Dist (mm)	<i>D_{max}</i> (Gy)		<i>D_{2%}</i> (Gy)		<i>D_{33%}</i> (Gy)		<i>D_{50%}</i> (Gy)		Γ_{pass}	Γ_{pass}
		Average	Motion	Average	Motion	Average	Motion	Average	Motion	3%/2mm/90%	3%/3mm/80%
C1*	63	16.44	16.08–16.67	13.84	13.47–13.85	1.05	1.04–1.25	0.58	0.59–0.64	0.71±0.16	0.73±0.07
C2*	66	10.36	9.86–10.73	9.09	8.82–9.15	1.57	1.17–3.05	0.55	0.50–0.69	0.85±0.12	0.81±0.08
C3*	65	11.45	11.01–11.41	9.21	9.16–9.74	0.28	0.25–0.29	0.15	0.14–0.17	0.50±0.32	0.62±0.24
C4*	66	37.70	35.69–39.54	30.17	28.33–30.31	13.90	10.29–13.81	1.36	1.53–1.92	0.78±0.14	0.88±0.04
C5*	56	16.03	16.04–16.55	14.62	14.59–14.88	5.57	4.67–6.78	0.68	0.65–0.71	0.90±0.08	0.85±0.05
C6*	58	24.57	22.68–25.02	17.88	17.12–18.65	3.15	2.37–3.60	1.08	0.57–1.18	0.84±0.05	0.85±0.04
C7*	79	18.71	17.86–19.69	15.29	14.90–15.87	6.75	6.19–7.72	0.94	0.87–1.09	0.78±0.07	0.84±0.03
C8*	65	9.18	9.86–10.56	8.08	8.65–9.08	0.42	0.44–0.55	0.21	0.18–0.28	0.93±0.06	0.74±0.05
C9*	38	7.14	5.84–7.19	6.06	4.99–5.99	0.37	0.30–0.43	0.23	0.20–0.24	0.99±0.04	0.76±0.06
C10*	50	10.96	10.42–11.32	9.62	9.45–9.70	5.90	4.04–6.44	0.71	0.51–0.85	0.95±0.04	0.86±0.05
C11*	100	8.49	8.15–8.42	7.50	7.32–7.49	0.40	0.35–0.40	0.24	0.21–0.25	0.96±0.06	0.73±0.05
Mean	64	15.55	15.42	12.85	12.80	3.58	3.37	0.61	0.63	0.84	0.79
SD	16	9.00	8.57	6.86	6.45	4.22	3.58	0.40	0.44	0.17	0.13
Max	100	37.70	39.54	30.17	30.31	13.90	13.81	1.36	1.92	0.99	0.88
Min	38	7.14	5.84	6.06	4.99	0.28	0.25	0.15	0.14	0.50	0.62

On average the maximal absolute change in position of the oesophageal border region was 4.24 ± 2.71 mm, 4.81 ± 2.58 mm and 10.21 ± 5.13 mm in LR, AP and SI direction, respectively (see table 1). What attracts attention is that there is a statistically significant difference between the two patient groups. For example, the TCIA cohort showed a mean maximal absolute motion (*MMAM*) of 7.46 ± 2.99 mm AP, whereas the internal patients exhibit a value of 3.61 ± 1.13 mm. We were able to measure a similar but less salient pattern in the other directions: The LR and SI *MMAM* were 3.61 ± 1.16 mm and 8.06 ± 4.03 mm for our internal patients compared to a *MMAM* of 5.64 ± 2.10 mm, 14.95 ± 4.12 mm for the TCIA patients.

In 7 out of 16 patients the maximum SI motion was measured in the lower part of the oesophagus in the area of the diaphragm. For the remaining 9 patients the SI maximum could be located either directly in the vicinity of the Carina or between Carina and diaphragm. Two LR maxima were located above the Carina, 5 at the height of the Carina, 5 between Carina and diaphragm and 4 in the lower part of the organ in the area of the diaphragm. In AP the location of the maximum positions was similar. In 3 cases the maximum was located above the Carina, 3 cases showed the maximum at the height of the Carina, 3 between Carina and diaphragm and 7 in the area of the diaphragm. An overview of motion amplitudes in connection with maxima positions is given by our motion model in 5.4.

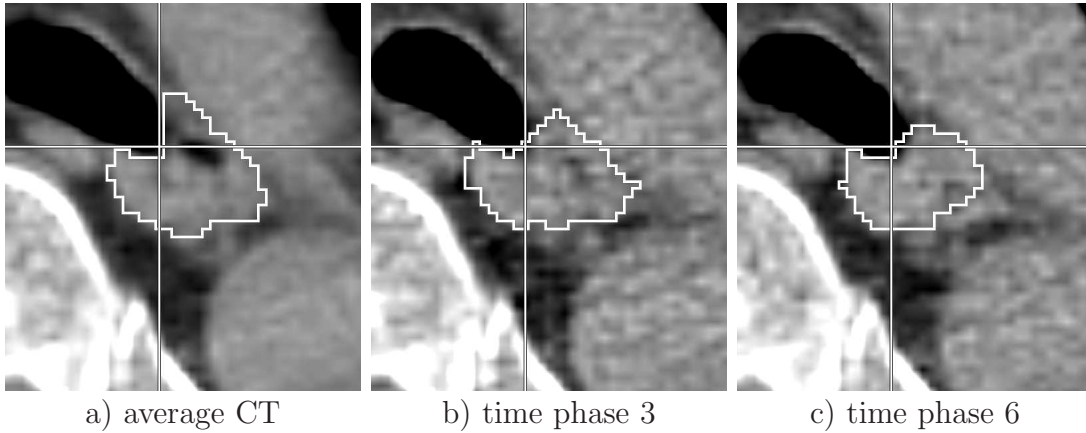


Figure 2: An illustration of the inconsistencies between contoured organ and real underlying motion for patient C4. With the use of the cross-hair it can be seen that the tissues moves from time phase 3 b) to time phase 6 c) towards the lower right image corner, but the shrinkage of the contour from time phase 3 to time phase 6 could be interpreted as an indicator for the opposite direction.

5.4. Oesophagus Motion Model

Figures 3 and 4 show the calculated motion model. The model contains the motion information from all 16 patients. The biggest movement can be expected in the lowest

part of the organ. The LR motion exhibits also a local maxima in the upper part of the organ around the Carina (Figure 4) which is in concordance with the findings in the *oesophagus motion and dose analysis* experiments. The average motion in LR and AP direction reside around 2 mm, for SI movement the average lies between 2 and 4 mm. However, the maximum motion can be much higher: up to 8 mm in LR and AP direction and up to 16 mm in SI direction. The fact that the patient-wise measured maxima are above the maxima of the model is because of two reasons: First, for the model we used the motion information from one time-phase contour, a maxima that was e.g. measured with the contour of a different time phase is therefore not reflected in the model. Second, the motion analysis was conducted only in the border region of the oesophagus and deviations in the DVF might map the maxima to a voxel outside the border region on the reference case. However, we analysed the DVFs for motion measurement before and after mapping to the reference case and could see only slight changes in the motion distribution (the maxima changed by 0.27 mm, 0.33 mm and 1.41 mm in LR, AP and SI direction, respectively).

6. Discussion

In this work we proposed a new method to measure oesophageal motion voxel-wise on 4DCT datasets taking into account the periodic breathing motion pattern. With this method we were able to analyse the organ motion for 16 patients and inspected possible under or over dosage of the oesophagus due to its movement. Additionally we scrutinised the delineation of the oesophagus on average CT and compared it to contouring on 4DCT. In a final step we showed how to create a motion model that facilitates an easier analysis, illustration and comparison of oesophageal motion on a voxel level across patients.

The results of our first experiment showed that the contour on average CT does not cover the whole organ and that a big part of the oesophagus resides outside the contour created on the average CT for a significant amount of time. This bears the risk of delivering too much dose to the oesophagus during treatment which could harm especially the radio-sensitive mucosa. The quantification of this motion in our second experiment showed that breathing induced LR MMAM, which is especially of interest for SBRT of the lungs, is over 5 mm for one cohort on average. This value is much higher than in other publications (Kobayashi et al. 2016, Gao et al. 2019, Sekii et al. 2018, Yaremko et al. 2008, Doi et al. 2018), solely Cohen et al. (2010) reported a similar value. Whereas Cohen et al. (2010) reported a lower value (2.8 mm) AP compared to the 4.81 mm of our experiments. A possible explanation of the different values could be that we used DIR and examined the whole organ whereas most other studies used rigid registration, centroid measurements or investigated only a smaller part of the organ. Another point is that the patient cohorts in the literature encompass mostly oesophageal cancer patients, where the tumour could reduce the mobility of the oesophagus. The work by Weiss et al. (2008) examined lung cancer patients and

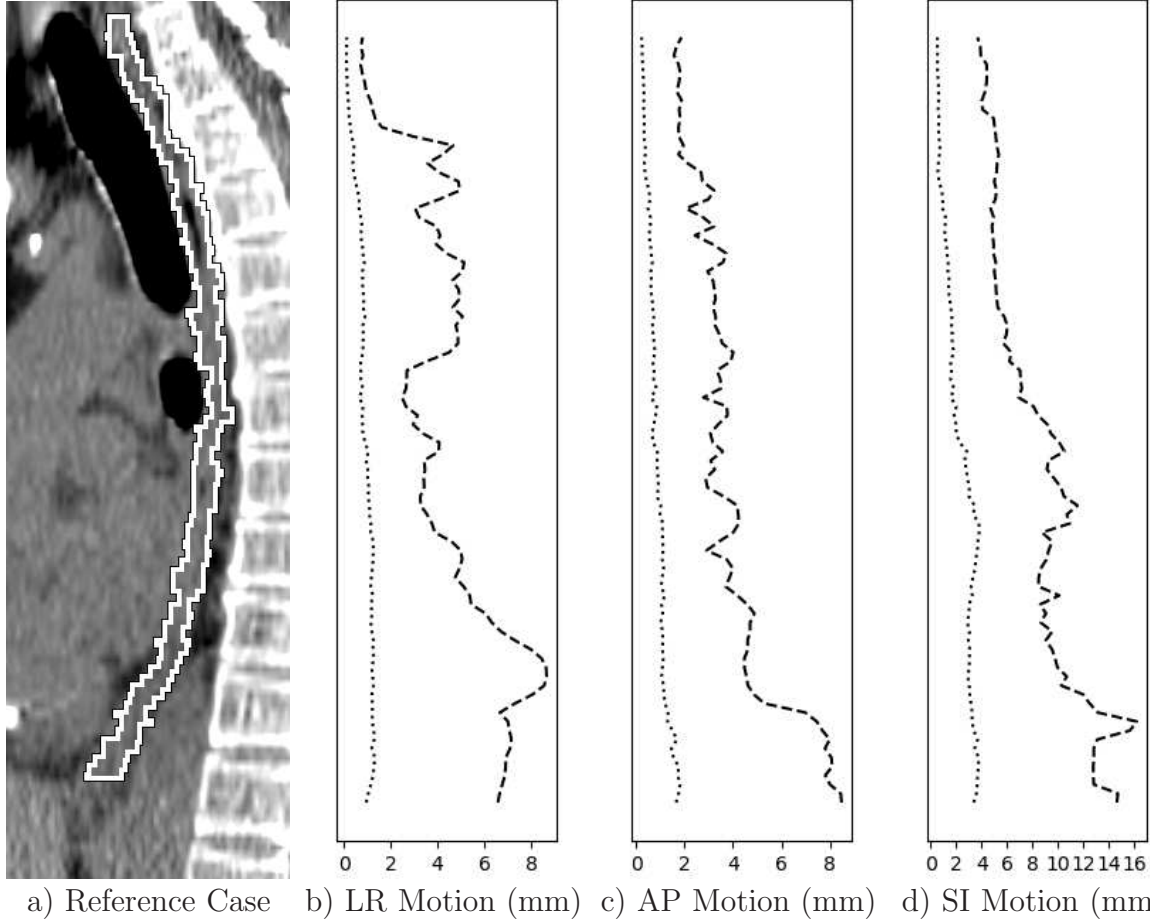


Figure 3: In a) the sagittal view of the reference case T1 with delineated oesophagus is shown. b) to d) illustrate maximum (dashed) and average (dotted) motion of our model in LR, AP and SI direction at the respective height of the organ. The model was generated by mapping the motion vector fields of all patients to the reference case

reported an average motion amplitude in axial plane comparable to the one of our internal cohort. Interestingly we experienced a gap in motion amplitudes between our two patient cohorts. An explanation for the different motion amplitudes in our internal and the TCIA cohort could be that the TCIA cohort consists mainly of locally advanced NSCLC with mediastinum infiltration, which is not the case for our internal cohort. Why oesophageal cancer patients show little motion compared to NSCLC patients with infiltrated mediastinum can only be speculated about: maybe huge larger lymph-nodes or tumour infiltration of locally advanced NSCLC in the mediastinum lead to displacement effects, that increase the mobility of the oesophagus during the breathing cycle while infiltrating oesophagus tumours might be more likely to fix the organ to the mediastinum. Summarized, our motion and contouring analysis suggests that oesophageal motion is heterogeneous and should be measured individually by using timely resolved imaging.

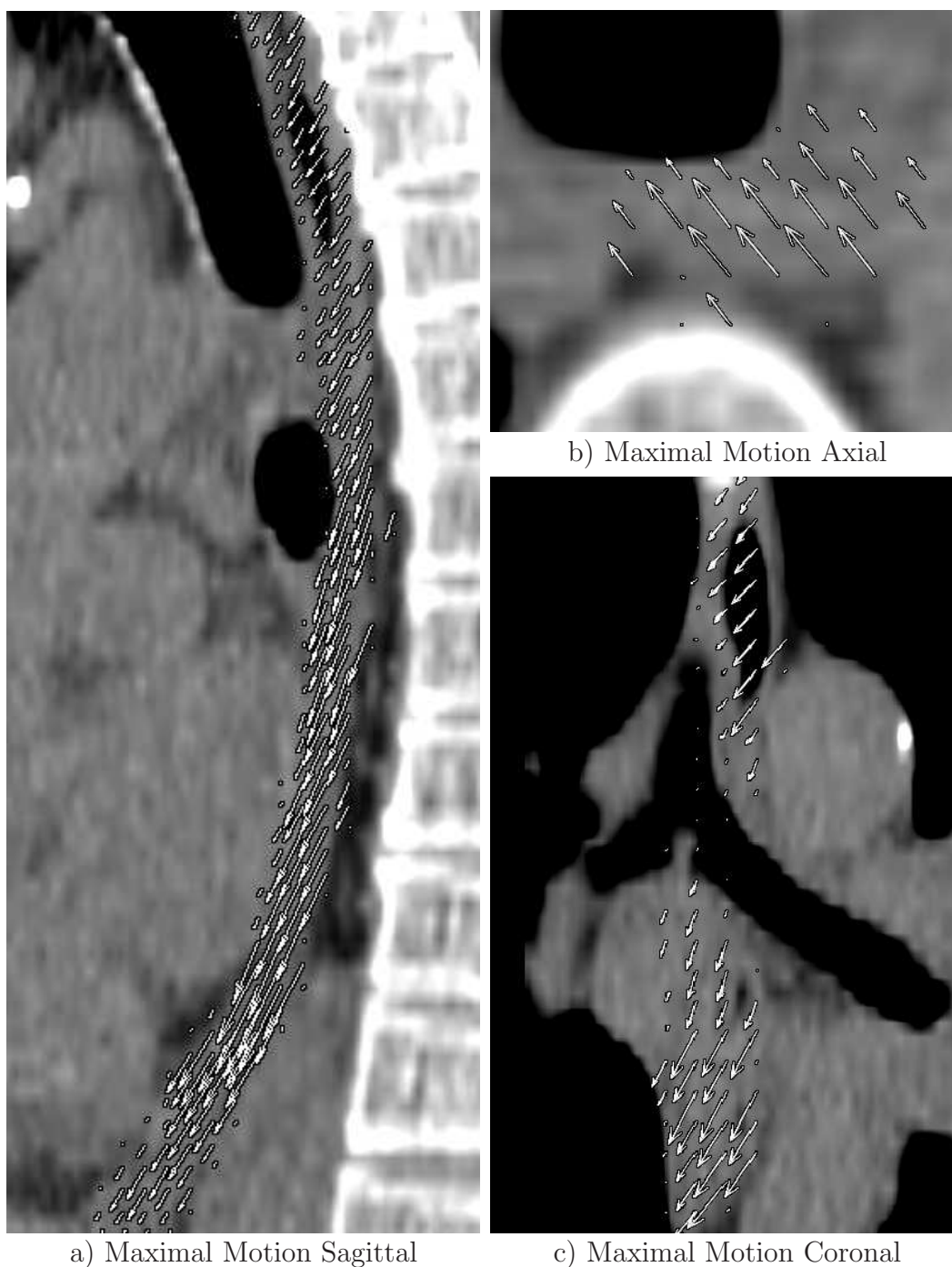


Figure 4: The reference case T1 of the created motion model shown in sagittal a), axial b) and coronal c) view. The overlaid arrows indicate the maximal motion of the model. The motion model contains the oesophageal motion information of all 16 patients.

The dose analysis showed that the absolute dose differences between the dose calculated on average CT and the motion corrected dose were all below or equal 2 Gy. At this point it is important to note that the mean distances of the oesophagus

to the dose maximum was 64 mm and the average maximum dose inside the oesophagi around 15 Gy. A treatment of tumours closer the oesophagus and higher dose gradients in the vicinity of the organ would probably increase the difference between planned and motion corrected dose. In approximately 50 % of the cases the passing-rate gamma criterion was not fulfilled which could be an indication for severe deviations from the planned dose. Additionally, for almost one fifth of the patients the maximum dose calculated on the average CT was not within the 95 % confidence interval of the motion corrected maximum dose. Although the results are connected to uncertainties from e.g. segmentation, registration or dose calculations, the trends seen in the results in combination with the actions we took to reduce the influence of those uncertainties (as discussed later on) might indicate that oesophageal motion should be considered also in the planning process.

With the created motion model, which encompasses the information from all patients we are able to illustrate the spatial motion distribution precisely for our two cohorts. The model shows that the maximum, especially for movement in the axial plane can be located around the Carina. Other studies split the oesophagus in different areas for motion analysis. Often the Carina was used as a boundary for those areas (Cohen et al. 2010, Sekii et al. 2018, Doi et al. 2018), maxima located above and below the Carina or in its direct vicinity could lead to averaging out and underestimating the motion.

Factors of uncertainty in our experiments are the created oesophagus demarcations and the image registration matrices and DVFs. Figure 2 shows that although we double checked every contour, inconsistencies due to misinterpretations can never be fully excluded. We tackled this issue by repeating the experiments for motion and dose inspection for each time phase image separately. The influence of registration or contouring mistakes is lowered by averaging over all time phase images. Also the extra QA of our registration algorithm and the comparison of the motion model amplitudes with the motion amplitudes of the original datasets are actions we took to lower uncertainty and improve the quality of our results.

We are aware of the relatively small number of patients enrolled in this study, and results need to be seen cautiously. By further improving our algorithms we are confident that we will be able to reduce the high amount of work necessary for the presented analysis, and are able to extend our study by more patients, including such with tumours in proximity to the oesophagus, where dose differences due to oesophageal movements might be more relevant, in the near future.

7. Conclusion

In this work we investigated the breathing induced motion of the oesophagus for central NSCLC patients. We compared the current clinical practice of contouring the oesophagus on 3DCT to timely resolved delineations and measured the impact of the motion on the delivered dose. Additionally, we build a motion model, encompassing

motion information from all patients, for a voxel-wise illustration of the motion along the whole organ. Our results showed that 4D information should be considered in the contouring process and that motion impacts the delivered dose. The experiments further showed that high motion amplitudes are not limited to the regions around the diaphragm, vary between patients and should be measured individually for each patient. Summarised, the numbers and tools presented in this work can mitigate motion related uncertainties, which might facilitate, in combination with additional experiments that further prove our initial results, SBRT closer to the mediastinal region.

Disclosure of Conflicts of Interest: The authors have no relevant conflicts of interest to disclose.

References

- Adebahr, S., Collette, S., Shash, E., Lambrecht, M., Le Pechoux, C., Faivre-Finn, C., De Ruyscher, D., Peulen, H., Belderbos, J., Dziadziuszko, R., Fink, C., Guckenberger, M., Hurkmans, C. & Nestle, U. (2015). LungTech, an EORTC Phase II trial of stereotactic body radiotherapy for centrally located lung tumours: a clinical perspective, *Br J Radiol* **88**(1051): 20150036.
- Cai, W., Hurwitz, M. H., Williams, C. L., Dhou, S., Berbeco, R. I., Seco, J., Mishra, P. & Lewis, J. H. (2015). 3d delivered dose assessment using a 4dct-based motion model, *Medical Physics* **42**(6Part1): 2897–2907.
URL: <https://aapm.onlinelibrary.wiley.com/doi/abs/10.1118/1.4921041>
- Castillo, E., Castillo, R., Martinez, J., Shenoy, M. & Guerrero, T. (2009). Four-dimensional deformable image registration using trajectory modeling, *Physics in Medicine & Biology* **55**(1): 305.
- Castillo, R., Castillo, E., Guerra, R., Johnson, V. E., McPhail, T., Garg, A. K. & Guerrero, T. (2009). A framework for evaluation of deformable image registration spatial accuracy using large landmark point sets, *Physics in Medicine & Biology* **54**(7): 1849.
- Chung, H., Jung, J., Jeong, C., Kwak, J., Park, J.-h., Kim, S. S., Yoon, S. M., Song, S. Y., Kim, J. H., Choi, E. K., Cho, S. & Cho, B. (2018). Evaluation of delivered dose to a moving target by 4d dose reconstruction in gated volumetric modulated arc therapy, *PLOS ONE* **13**: 1–18.
URL: <https://doi.org/10.1371/journal.pone.0202765>
- Clark, K., Vendt, B., Smith, K., Freymann, J., Kirby, J., Koppel, P., Moore, S., Phillips, S., Maffitt, D., Pringle, M., Tarbox, L. & Prior, F. (2013). The cancer imaging archive (TCIA): Maintaining and operating a public information repository, *Journal of Digital Imaging* **26**(6): 1045–1057.
URL: <https://doi.org/10.1007/s10278-013-9622-7>
- Cohen, R. J., Paskalev, K., Litwin, S., Price, R. A., J., Feigenberg, S. J. & Konski, A. A. (2010). Esophageal motion during radiotherapy: quantification and margin implications, *Diseases of the Esophagus* **23**(6): 473–479.
URL: <https://doi.org/10.1111/j.1442-2050.2009.01037.x>
- Collier, D. C., Burnett, S. S. C., Amin, M., Bilton, S., Brooks, C., Ryan, A., Roniger, D., Tran, D. & Starkschall, G. (2003). Assessment of consistency in contouring of normal-tissue anatomic structures, *Journal of Applied Clinical Medical Physics* **4**(1): 17–24.
URL: <https://aapm.onlinelibrary.wiley.com/doi/abs/10.1120/jacmp.v4i1.2538>
- Doi, Y., Murakami, Y., Imano, N., Takeuchi, Y., Takahashi, I., Nishibuchi, I., Kimura, T. & Nagata, Y. (2018). Quantifying esophageal motion during free-breathing and breath-hold using fiducial markers in patients with early-stage esophageal cancer, *PLoS ONE* **13**(6): e0198844.
- Ehrbar, S., Lang, S., Stieb, S., Riesterer, O., Stark, L. S., Guckenberger, M. & Klöck, S. (2016). Three-dimensional versus four-dimensional dose calculation for volumetric modulated arc therapy of

- hypofractionated treatments, *Zeitschrift für Medizinische Physik* **26**(1): 45 – 53.
URL: <http://www.sciencedirect.com/science/article/pii/S0939388915000720>
- Fechter, T., Adebahr, S., Baltas, D., Ben Ayed, I., Desrosiers, C. & Dolz, J. (2017). Esophagus segmentation in ct via 3d fully convolutional neural network and random walk, *Medical Physics* **44**(12): 6341–6352.
URL: <https://aapm.onlinelibrary.wiley.com/doi/abs/10.1002/mp.12593>
- Fechter, T. & Baltas, D. (2020). One-shot learning for deformable medical image registration and periodic motion tracking, *IEEE Transactions on Medical Imaging* **39**(7): 2506–2517.
- Fedorov, A., Beichel, R., Kalpathy-Cramer, J., Finet, J., Fillion-Robin, J.-C., Pujol, S., Bauer, C., Jennings, D., Fennessy, F., Sonka, M., Buatti, J., Aylward, S., Miller, J. V., Pieper, S. & Kikinis, R. (2012). 3d slicer as an image computing platform for the quantitative imaging network, *Magnetic Resonance Imaging* **30**(9): 1323 – 1341. Quantitative Imaging in Cancer.
URL: <http://www.sciencedirect.com/science/article/pii/S0730725X12001816>
- Gao, H., Kelsey, C. R., Boyle, J., Xie, T., Catalano, S., Wang, X. & Yin, F. F. (2019). Impact of Esophageal Motion on Dosimetry and Toxicity With Thoracic Radiation Therapy, *Technol. Cancer Res. Treat.* **18**: 1533033819849073.
- Han, C., Yu, W., Zheng, X., Zhou, Y., Gong, C., Xie, C. & Jin, X. (2018). Composite QA for intensity-modulated radiation therapy using individual volume-based 3D gamma indices, *Journal of Radiation Research* **59**(5): 669–676.
- Hugo, G. D., Weiss, E., Sleeman, W. C., Balik, S., Keall, P. J., Lu, J. & Williamson, J. F. (2016). Data from 4d lung imaging of nscl patients.
URL: <https://wiki.cancerimagingarchive.net/x/1oNEAQ>
- Hussein, M., Clark, C. & Nisbet, A. (2017). Challenges in calculation of the gamma index in radiotherapy – towards good practice, *Physica Medica* **36**: 1 – 11.
URL: <http://www.sciencedirect.com/science/article/pii/S1120179717300558>
- Isensee, F., Petersen, J., Kohl, S. A. A., Jäger, P. F. & Maier-Hein, K. H. (2019). nnu-net: Breaking the spell on successful medical image segmentation, *CoRR* **abs/1904.08128**.
URL: <http://arxiv.org/abs/1904.08128>
- Klein, S., Staring, M., Murphy, K., Viergever, M. A. & Pluim, J. P. W. (2010). elastix: A toolbox for intensity-based medical image registration, *IEEE Transactions on Medical Imaging* **29**(1): 196–205.
- Kobayashi, Y., Myojin, M., Shimizu, S. & Hosokawa, M. (2016). Esophageal motion characteristics in thoracic esophageal cancer: Impact of clinical stage T4 versus stages T1-T3, *Adv Radiat Oncol* **1**(4): 222–229.
- Kong, F. M., Ritter, T., Quint, D. J., Senan, S., Gaspar, L. E., Komaki, R. U., Hurkmans, C. W., Timmerman, R., Bezjak, A., Bradley, J. D., Movsas, B., Marsh, L., Okunieff, P., Choy, H. & Curran, W. J. (2011). Consideration of dose limits for organs at risk of thoracic radiotherapy: atlas for lung, proximal bronchial tree, esophagus, spinal cord, ribs, and brachial plexus, *Int J Radiat Oncol Biol Phys* **81**(5): 1442–1457.
- Lambert, Z., Petitjean, C., Dubray, B. & Ruan, S. (2019). Segthor: Segmentation of thoracic organs at risk in ct images.
- Low, D. A., Harms, W. B., Mutic, S. & Purdy, J. A. (1998). A technique for the quantitative evaluation of dose distributions, *Medical Physics* **25**(5): 656–661.
URL: <https://aapm.onlinelibrary.wiley.com/doi/abs/10.1118/1.598248>
- Miften, M., Olch, A., Mihailidis, D., Moran, J., Pawlicki, T., Molineu, A., Li, H., Wijesooriya, K., Shi, J., Xia, P., Papanikolaou, N. & Low, D. A. (2018). Tolerance limits and methodologies for IMRT measurement-based verification QA: Recommendations of AAPM Task Group No. 218, *Med Phys* **45**(4): e53–e83.
- Palmer, J., Yang, J., Pan, T. & Court, L. E. (2014). Motion of the esophagus due to cardiac motion, *PLoS ONE* **9**(2): e89126.
- Patel, A. A., Wolfgang, J. A., Niemierko, A., Hong, T. S., Yock, T. & Choi, N. C. (2009).

- Implications of respiratory motion as measured by four-dimensional computed tomography for radiation treatment planning of esophageal cancer, *International Journal of Radiation Oncology*Biophysics* **74**(1): 290 – 296.
URL: <http://www.sciencedirect.com/science/article/pii/S0360301609000066>
- Report 83 (2016). *Journal of the International Commission on Radiation Units and Measurements* **10**(1): NP–NP.
URL: <https://doi.org/10.1093/jicru/10.1.Report83>
- Rouabhi, O., Ma, M., Bayouth, J. & Xia, J. (2015). Impact of temporal probability in 4d dose calculation for lung tumors, *Journal of applied clinical medical physics* **16**(6): 110—118.
URL: <https://europepmc.org/articles/PMC5691019>
- Sekii, S., Ito, Y., Harada, K., Kitaguchi, M., Takahashi, K., Inaba, K., Murakami, N., Igaki, H., Sasaki, R. & Itami, J. (2018). Intrafraction esophageal motion in patients with clinical T1N0 esophageal cancer, *Rep Pract Oncol Radiother* **23**(5): 398–401.
- Sørensen, T. (1948). *A Method of Establishing Groups of Equal Amplitude in Plant Sociology Based on Similarity of Species Content and Its Application to Analyses of the Vegetation on Danish Commons*, Biologiske skrifter, I kommission hos E. Munksgaard.
URL: <https://books.google.de/books?id=rpS8GAAACAAJ>
- Timmerman, R., McGarry, R., Yiannoutsos, C., Papiez, L., Tudor, K., DeLuca, J., Ewing, M., Abdulrahman, R., DesRosiers, C., Williams, M. & Fletcher, J. (2006). Excessive toxicity when treating central tumors in a phase ii study of stereotactic body radiation therapy for medically inoperable early-stage lung cancer, *Journal of Clinical Oncology* **24**(30): 4833–4839. PMID: 17050868.
- Vandemeulebroucke, J., Rit, S., Kybic, J., Clarysse, P. & Sarrut, D. (2011). Spatiotemporal motion estimation for respiratory-correlated imaging of the lungs, *Medical physics* **38**(1): 166–178.
- Wang, X., Yang, J., Zhao, Z., Luo, D., Court, L., Zhang, Y., Weksberg, D., Brown, P. D., Li, J. & Ghia, A. J. (2019). Dosimetric impact of esophagus motion in single fraction spine stereotactic body radiotherapy, *Physics in Medicine & Biology* **64**(11): 115010.
- Weiss, E., Wijesooriya, K. & Keall, P. (2008). Esophagus and spinal cord motion relative to gtv motion in four-dimensional cts of lung cancer patients, *Radiotherapy and Oncology* **87**(1): 44 – 48.
URL: <http://www.sciencedirect.com/science/article/pii/S0167814007006664>
- Yang, J., Veeraraghavan, H., Armato, S. G., Farahani, K., Kirby, J. S., Kalpathy-Kramer, J., van Elmpt, W., Dekker, A., Han, X., Feng, X., Aljabar, P., Oliveira, B., van der Heyden, B., Zamdborg, L., Lam, D., Gooding, M. & Sharp, G. C. (2018). Autosegmentation for thoracic radiation treatment planning: A grand challenge at AAPM 2017, *Med Phys* **45**(10): 4568–4581.
- Yaremko, B. P., Guerrero, T. M., McAleer, M. F., Bucci, M. K., Noyola-Martinez, J., Nguyen, L. T., Balter, P. A., Guerra, R., Komaki, R. & Liao, Z. (2008). Determination of respiratory motion for distal esophagus cancer using four-dimensional computed tomography, *Int. J. Radiat. Oncol. Biol. Phys.* **70**(1): 145–153.